Instability of Spinning Projectiles During Terminal Guidance

K.H. Lloyd* and D.P. Brown†
Australian Defence Scientific Service, Weapons Systems Research Laboratory, Salisbury, South Australia

We examine the criteria for dynamic stability of a spinning projectile subjected to steady horizontal and vertical side forces applied at the nose; such forces could, for example, be generated by canards mounted on a roll-stabilized nose. The problem requires an extension of standard aeroballistic theory which yields intersting new information on stability. It is found that the precessional and nutational modes can become unstable, depending on the magnitude and direction of the applied side force. Results of numerical simulations which confirm these conclusions are given.

Nomenclature

C_{lp} = roll damping moment coefficient derivative
$C_{m\alpha}$ = pitching moment coefficient derivative
C_{mq} = pitch damping moment coefficient derivative
$C_{N\alpha}$ = normal force coefficient derivative
$C_{np\alpha}$ = Magnus moment coefficient derivative
C_x = axial force coefficient
$C_{Y_{p\alpha}}$ = Magnus force coefficient derivative
F_y = applied control force in horizontal direction
F_z = applied control force in vertical plane
I_{xx} = moment of inertia about x axis
I_{yy} = moment of inertia about y and z axes
M_w = pitching moment derivative
M_q = pitch damping moment derivative
N_{pw} = Magnus moment derivative
p = projectile roll rate
p_a = roll rate of axes system ($=-r\tan\theta$ in aeroballistic axes, $=0$ in nonspinning axes)
q,r = angular velocity about y and z axes
u,v,w = velocity components
V = total projectile velocity
X = distance of application of control force forward from center of gravity
Z_w = normal force derivative
α,β = angles of attack and sideslip
λ = damping rate (real part of eigenvalue)
θ = Euler elevation angle of the projectile spin axis
ϕ = residual roll angle of nonspinning axes
ψ = eigenvalues of motion
ω = frequency (imaginary part of eigenvalue)

I. Introduction

In recent digital computer simulations of the flight of terminally guided spinning projectiles it was observed that side forces applied at the nose sometimes lead to precessional or nutational instability. In these simulations, the nose was assumed to be free to roll relative to the spinning projectile and its roll orientation was controlled relative to Earth. Since this result is not predicted by the traditional linear theory of shell stability, and to verify that it was not simply caused by an incorrect numerical procedure, we have re-examined the shell stability theory. It turns out the result is predictable by a linear theory provided that, before linearization, the exact equations of motion are expressed in what we prefer to distinguish as "nonspinning axes" ($p_a=0, \phi\neq 0$), rather than in aeroballistic axes ($p_a=-r\tan\theta, \phi=0$).

Nicolaides[1] and Murphy[2] have contributed significantly to the study of the stability of spinning projectiles, and their results are those most frequently quoted today. Both these workers not only linearized the equations of motion but also assumed that the flight path was almost horizontal in order to further simplify the equations. When this assumption is made, the distinction between the nonspinning and aeroballistic axes systems disappears; the effects of gravity and applied side forces produced, for example, by canards (Regan and Smith[3]) then do not enter into the derived criteria for dynamic stability. It is because we are concerned here with both arbitrary flight path elevation angles and with side forces comparable with the projectile's weight that the usual approximations become inadequate. The dynamic instability discussed is associated with these conditions and so is additional to the classical gyroscopic and dynamic instabilities of unguided spinning projectiles discussed, for example, by Nicolaides.[1]

By expressing the equations of motion in nonspinning axes and then linearizing, but without assuming that the flight path elevation angle is small, we obtain a system of six first-order ordinary differential equations, the solution of which reveals the influence of side forces and gravity on dynamic stability. The equations are solved as an eigenvalue problem, yielding expressions for nutational and precessional damping rates and frequencies. The additional mode described by our sixth-order system of equations, which we shall call the $\theta-\phi$ mode, is related to curvature of the trajectory.

In Sec. II we present the equations of motion, first in aeroballistic axes and then transformed to nonspinning axes. We have used time as the independent variable rather than distance along the trajectory as is often done, since it simplifies the present analysis. This wish to refrain from needlessly complicating the treatment with terms that produce negligible effect on stability has also resulted in our excluding Magnus force (however, Magnus moment cannot be neglected). The effects of the neglected terms are adequately discussed by Nicolaides.[1]

Section III solves the linearized equations of motion as an eigenvalue problem and Sec. IV evaluates the stability criteria from the derived eigenvalues. It is found that the motion of a typical 105-mm shell, having a mass of 15 kg, remains stable provided the horizontal component of the control force, when applied at the nose, remains less than about 50 N (equivalent to an acceleration of 0.34 g). For larger side forces, either nutational or precessional instability may be produced, depending upon the Euler elevation angle (θ, see Fig. 1) and whether the force is toward the right or left of the trajectory. On the downleg, for example, assuming that the shell spin is

Received Dec. 27, 1977; revision received July 25, 1978.

Index category: LV/M Dynamics and Control.

*Senior Research Scientist, Flight Research Group, Aeroballistics Division.

†Research Scientist, Flight Research Group, Aeroballistics Division.

clockwise when viewed from the rear, a horizontal force to the right applied at the nose tends to stabilize precession and destabilize nutation, while a force to the left tends to destabilize precession and stabilize nutation. The opposite occurs on the downleg or if the sense of shell rotation is reversed and the effect diminishes as the elevation approaches zero. Instability with vertical control foces, applied at the nose, does not occur unless the force exceeds an unrealistically large 1000 N (producing almost 7 g). The effect of gravity on dynamic stability is also very small.

Finally, Sec. V gives results of numerical solutions of the equations of motion. These agree fairly well with the analytic solution.

II. Equations of Motion

The axes systems used in formulating the problem are illustrated in Fig. 1. In addition to the standard aerodynamic forces and gravity, the spinning projectile is also subjected to a lateral control force, applied a distance X forward from the center of gravity, with components F_y and F_z as indicated in Fig. 1. Such a force could be applied, for example, by canards mounted on the nose, the nose being mechanically decoupled in roll from the projectile and roll-stabilized relative to Earth.

The equations of motion will first be written in aeroballistic axes, the angular velocity of which is (p_a, q, r) with $p_a = -r\tan\theta$; p_a is the roll rate necessary to keep the y axis horizontal. The x axis lies along the projectile spin axis, y lies to the right in a horizontal plane and z in a vertical plane. These axes are often preferred because they represent quantities in a way which is easily understood by a ground-based observer. Neglecting changes in spin rate and axial velocity, which are small and inconsequential to our problem, assuming small incidence, and letting $u = V$, the equations of motion in aeroballistic axes can be written as (see, for example, Kolk[4]):

$$\dot{v} = Z_w v - Vr - (r\tan\theta)\, w + F_y/m \tag{1}$$

$$\dot{w} = Z_w w + Vq + (r\tan\theta)\, v + g\cos\theta + F_z/m \tag{2}$$

$$\dot{q} = N_{pw} v/V + M_w w/V + M_q q - (pI_{xx}/I_{yy})\, r - (r\tan\theta)\, r - X = F_z/I_{yy} \tag{3}$$

$$\dot{r} = -M_w v/V + N_{pw} w/V + (pI_{xx}/I_{yy})\, q + M_q r + (r\tan\theta)\, q + XF_y/I_{yy} \tag{4}$$

where the aerodynamic force and moment derivatives are given by:

$$M_w = \tfrac{1}{2}\rho V^2 SdC_{m\alpha}/I_{yy}$$

$$Z_w = \tfrac{1}{2}\rho V^2 SC_{N\alpha}/mV$$

$$M_q = \tfrac{1}{2}\rho V^2 Sd(d/2V)\, C_{mq}/I_{yy}$$

$$N_{pw} = \tfrac{1}{2}\rho V^2 Sd(pd/2V)\, C_{np\alpha}/I_{yy}$$

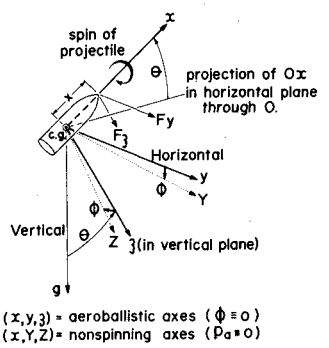

Fig. 1 Axes systems.

Because of the factors $(r\tan\theta)$ and $\cos\theta$, Eqs. (1-4) are nonlinear. If F_y is sufficiently small and $\tan\theta$ is not large, the terms involving $r\tan\theta$ are small, and a linearization which neglects them is a good approximation, particularly if the elevation angle θ is small. When this approximation is made, however, the control force components F_y and F_z merely produce a trim change and do not affect the projectile's dynamic stability, contrary to our numerical experiences for cases where F_y is not small. Neglecting the terms containing $(r\tan\theta)$ is equivalent to neglecting the roll rate $(p_a = -r\tan\theta)$ which is necessary to keep the y axis of the aeroballistic axes horizontal as the projectile pitches and yaws. These linearized equations, therefore, refer strictly to nonspinning axes $(p_a = 0)$, but they then incorrectly imply that F_y, F_z, and g act in a constant direction in this axes system, which can introduce significant errors. This suggests that one should start with the exact equations of motion in nonspinning axes and then linearize them to obtain a set of equations which, to first order, correctly allow for the variation in the direction of F_y, F_z, and g in these axes.

Transforming Eqs. (1-4) into the nonspinning axes system is effected by rotation about the x axis by the angle ϕ, where $\phi = \int(r\cos\phi + q\sin\phi)\tan\theta\, dt$ is the change of Euler roll angle suffered by the nonspinning axes. Making this transformation and introducing the (small) angles of attack $\alpha = w/V$ and sideslip $\beta = v/V$ gives:

$$\dot{\beta} = Z_w\beta - r + (g\cos\theta_0/V + F_z/mV)\phi + F_y/mV \tag{5}$$

$$\dot{\alpha} = Z_w\alpha + q - (F_y/mV)\phi - (g\sin\theta_0/V)\theta + g\cos\theta_0/V + F_z/mV \tag{6}$$

$$\dot{q} = N_{pw}\beta + M_w\alpha + M_q q - (pI_{xx}/I_{yy})\, r + (XF_y/I_{yy})\phi - XF_z/I_{yy} \tag{7}$$

$$\dot{r} = -M_w\beta + N_{pw}\alpha + (pI_{xx}/I_{yy})\, q + M_q r + (XF_z/I_{yy})\phi + XF_y/I_{yy} \tag{8}$$

To complete this set of equations we need a pair of equations for the rates of change of θ and ϕ. These are given to first order by

$$\dot{\theta} = q \tag{9}$$

$$\dot{\phi} = r\tan\theta_0 \tag{10}$$

Note that the variables are now with respect to the nonspinning axes. In deriving Eqs. (5-10) we have assumed ϕ is small, so we have put $\cos\phi = 1$, $\sin\phi = \phi$, and have neglected products such as $r\phi$ and $q\phi$. The validity of this assumption will be discussed later. Note that there is no loss of generality in assuming that $\phi = 0$ initially. We also assumed that the interval being considered is sufficiently short that variations in θ are small, thereby replacing θ by $(\theta_0 + \theta)$, where θ is now the departure from its initial value, θ_0; this typically restricts the time interval to a few seconds.

It is interesting to note that linearization of the transformed equations is not equivalent to transformation of the linearized equations. Essentially, $r\tan\theta$ in Eqs. (1-4) is not negligible if F_y is large and θ is arbitrary, and by writing the equations in nonspinning axes we are able to avoid having to assume F_y and θ are small in order to linearize the equations.

III. Solution of the Linearized Equations

Equations (5-10) are six linear first-order equations in the six variables β, α, q, r, θ, ϕ. Since the coefficients are constants, the solution can be expressed as the sum of six terms of the form

$$x_j = x_{0j}\exp(\psi_j t) \qquad j = 1,6$$

Table 1 Coefficients of eigenvalue Eq. (11)

Multiples	Cofficient a_3	a_4	a_5	a_6
1	$-2(Z_w pI_{xx}/I_{yy} - N_{pw})pI_{xx}/I_{yy}$ $-2(M_q + Z_w)(M_q Z_w - M_w)$	$(M_q Z_w - M_w)^2$ $+(Z_w pI_{xx}/I_{yy} - N_{pw})^2$	...	...
$F_y \tan\theta_0/mV$	N_{pw}	$M_w pI_{xx}/I_{yy} - N_{pw}(M_q + Z_w)$	$-Z_w(M_w pI_{xx}/I_{yy} - N_{pw}M_q)$	...
$XF_y \tan\theta_0/I_{yy}$	$-pI_{xx}/I_{yy}$	$2Z_w pI_{xx}/I_{yy} - N_{pw}$	$-Z_w(Z_w pI_{xx}/I_{yy} - N_{pw})$	$-N_{pw}Z_w g \sin\theta_0/V$
$F_z \tan\theta_0/mV$	M_w	$-M_w(M_q + Z_w) - N_{pw}pI_{xx}/I_{yy}$	$-(M_w^2 + N_{pw}^2)$ $+Z_w(N_{pw}pI_{xx}/I_{yy} + M_w M_q)$	$(M_w^2 + N_{pw}^2) g \sin\theta_0/V$
$XF_z \tan\theta_0/I_{yy}$	$M_q + 2Z_w$	$-M_w - Z_w(M_q + 2Z_w)$	$-Z_w(M_w - M_q Z_w)$	$M_w Z_w g \sin\theta_0/V$
$g \sin\theta_0/V$	$2M_w$	$-2M_w(M_q + Z_w) - 2N_{pw}pI_{xx}/I_{yy}$	$-2(M_w^2 + N_{pw}^2)$ $+2Z_w(N_{pw}pI_{xx}/I_{yy} + M_w M_q)$	$(M_w^2 + N_{pw}^2) g \sin\theta_0/V$
$g \sin\theta_0 \tan\theta_0$	...	...	$(N_{pw}F_y - M_w F_z)X/I_{yy}$	...

Table 2 Typical values for parameters[a]

V	= 250 m/s	$C_{m\alpha}$	= 3.8
p	= 1050 rad/s	$C_{N\alpha}$	= −1.8
ρ	= 1.05 kg/m^3	C_{mq}	= −16
m	= 15 kg	$C_{np\alpha}$	= 0.4[b]
I_{xx}	= 0.023 kg m^2	M_w	= 500 s^{-2}
I_{yy}	= 0.22 kg m^2	Z_w	= −0.137 s^{-1}
d	= 0.105 m	M_q	= −0.457 s^{-1}
S	= 0.0087 m^2	N_{pw}	= 12 s^{-2}
X	= 0.3 m	F_y	= 0→100 N[c]
g	= 9.8 m/s^2	F_z	= 0→100 N[c]

[a] The values apply to halfway on the downleg of a 105-mm shell trajectory.
[b] Magnus moment increases rapidly from 0.02 to 1.0 in the transonic region. We have taken a mean value.
[c] Canards mounted on the nose are likely to produce side forces in this range.

Table 3 Effect of forces on normal modes

Force		Precession	Nutation
$F_y \tan\theta_0$	>0	Destabilizing	Stabilizing
	<0	Stabilizing	Destabilizing
$F_z \tan\theta_0$	>0	Stabilizing	Nil
	<0	Destabilizing	Nil
$g \sin\theta_0$	>0	Stabilizing	Nil
	<0	Destabilizing	Nil

θ_0 is positive on the upleg, F_y is positive to the right viewed from the rear, and F_z is positive downwards.

where ψ_j is the jth eigenvalue. The stability of a given mode depends on the sign of the real part of ψ_j.

Substituting x_j just given into Eqs. (5-10) gives six algebraic equations in the x_{0j}, which only have nontrivial solutions if the determinant of the coefficients is zero. Multiplying this determinant gives a sixth degree eigenvalue equation of the form:

$$\psi^6 + a_1\psi^5 + a_2\psi^4 + a_3\psi^3 + a_4\psi^2 + a_5\psi + a_6 = 0 \qquad (11)$$

where

$$a_1 = -2(M_q + Z_w)$$

$$a_2 = (pI_{xx}/I_{yy})^2 + 2(M_q Z_w - M_w) + (M_q + Z_w)^2 - XF_z \tan\theta_0/I_{yy}$$

and the other coefficients all have terms involving F_y, F_z, g, XF_y, and XF_z, so it is simplest to present them in tabular form, which is done in Table 1. Each coefficient is given by the summed product of the row headings with the table entry. Fortunately, for a typical spinning projectile, a few of the terms dominate and the others may be neglected. In Table 2 we have listed representative values for all the parameters in our problem. Using these values to determine the dominant terms, we obtain the following expressions correct to first order, for the coefficients of Eq. (11):

$$a_1 = -2(M_q + Z_w) \qquad (12)$$

$$a_2 = (pI_{xx}/I_{yy})^2 - 2M_w \qquad (13)$$

$$a_3 = -2(pI_{xx}/I_{yy})(Z_w pI_{xx}/I_{yy} - N_{pw}) + 2M_w(M_q + Z_w) - X(pI_{xx}/I_{yy}^2)F_y \tan\theta_0 \qquad (14)$$

$$a_4 = M_w^2 \qquad (15)$$

$$a_5 = -2M_w^2 g \sin\theta_0/V - (g \sin\theta_0/V + Z_w)(M_w X/I_{yy})F_z \tan\theta_0 \qquad (16)$$

$$a_6 = M_w^2(g \tan\theta_0/V)^2 + (M_w + Z_w Xm/I_{yy})(M_w/m)(g \sin\theta_0/V)F_z \tan\theta_0/V \qquad (17)$$

IV. Stability Criteria

The frequency and damping of the normal modes of the projectile's motion are given by the imaginary and real parts of the solutions of Eq. (11). Rather than attempt to attack this equation directly, we shall adopt an approach which makes use of the known properties of the solutions.

When gravity and side forces are not present, the eigenvalue equation reduces to a fourth degree one whose solution is well known, consisting of two pairs of complex conjugates. The motions corresponding to these are the precessional and nutational modes:

$$\psi_P = \lambda_P \pm i\omega_P \qquad \psi_N \pm i\omega_N \qquad (18)$$

whose relative magnitudes for a typical spinning projectile are:

$$\omega_N > \omega_P > 1, \quad |\lambda|_N \sim |\lambda|_P < 1$$

Introduction of Eqs. (9) and (10) increases the degree of the eigenvalue equation by two and so introduces two more roots, which we shall denote by $\psi_{\theta,\phi}$. These roots may either be a complex conjugate pair, or both real. For now, we shall assume they are of the form

$$\psi_{\theta,\phi} = \lambda_{\theta,\phi} \pm i\omega_{\theta,\phi} \qquad (19)$$

where $\omega_{\theta,\phi}$ is imaginary if the roots $\psi_{\theta,\phi}$ happen to be real. These roots tend to zero for vanishingly small values of $g\sin\theta_0$, F_y, and F_z, and as will be shown, they are always much less than unity.

Expressing the roots in this form, we can express the coefficients of Eq. (11) as sums and products of the ω's and λ's. By retaining only the dominant terms, these simplify to

$$a_1 = -2(\lambda_P + \lambda_N + \lambda_{\theta,\phi}) \tag{20}$$

$$a_2 = \omega_N^2 \tag{21}$$

$$a_3 = -2\omega_N^2(\lambda_P + \lambda_{\theta,\phi}) \tag{22}$$

$$a_4 = \omega_N^2\omega_P^2 \tag{23}$$

$$a_5 = -2\omega_N^2\omega_P^2\lambda_{\theta,\phi} \tag{24}$$

$$a_6 = \omega_N^2\omega_P^2(\lambda_{\theta,\phi}^2 + \omega_{\theta,\phi}^2) \tag{25}$$

From Eqs. (12-17) and Eqs. (20-25) we obtain expressions for the eigenvalues in terms of the parameters of the problem. First we confirm that $\lambda_{\theta,\phi}$ and $\omega_{\theta,\phi}$ are indeed small; from Eqs. (15-17) and Eqs. (23-25) we have

$$\lambda_{\theta,\phi} = g\sin\theta_0/V + (Z_w + g\sin\theta_0/V)(X/2M_wI_{yy})F_z\tan\theta_0 \tag{26}$$

$$\omega_{\theta,\phi}^2 = [(M_w - Xmg\sin\theta_0/I_{yy})/(M_wm)](g\sin\theta_0/V)F_z\tan\theta_0/V \tag{27}$$

Provided θ_0 is not close to $\pi/2$, the largest term in either of these expressions is $g\sin\theta_0/V$, which is of the order of 0.04.

Equations (13) and (21) give ω_N^2 immediately, and since $M_w \ll (pI_{xx}/I_{yy})^2$, it follows that

$$\omega_N = pI_{xx}/I_{yy} - M_wI_{yy}/pI_{xx} \tag{28}$$

correct to first order.

We can now calculate ω_P from Eqs. (15) and (23):

$$\omega_P = M_wI_{yy}/pI_{xx} + M_w^2(I_{yy}/pI_{xx})^3 \tag{29}$$

Also, from Eqs. (12, 14, 20, and 22) we have:

$$\begin{aligned}\lambda_N = {} & M_q + [1 + 2M_w(I_{yy}/pI_{xx})^2]N_{pw}I_{yy}/pI_{xx} \\ & + (M_q - Z_w)(I_{yy}/pI_{xx})^2M_w \\ & - (X/2pI_{xx})[1 + 2M_w(I_{yy}/pI_{xx})^2]F_y\tan\theta_0\end{aligned} \tag{30}$$

Finally, from Eqs. (14) and (22),

$$\begin{aligned}\lambda_P = {} & Z_w - [1 + 2M_w(I_{yy}/pI_{xx})^2]N_{pw}I_{yy}/pI_{xx} \\ & - (M_q - Z_w)(I_{yy}/pI_{xx})^2M_w \\ & + (X/2pI_{xx})[1 + 2M_w(I_{yy}/pI_{xx})^2]F_y\tan\theta_0 - g\sin\theta_0/V \\ & - (Z_w + g\sin\theta_0/V)(X/2M_wI_{yy})F_z\tan\theta_0\end{aligned} \tag{31}$$

In every case we have put the dominant terms first in the expressions on the right-hand side. When $F_y = F_z = g = 0$ these expressions reduce to the well-known solutions of the linearized equations of motion.[1] Pitch damping and normal force are the prime stabilizing factors for nutation and precession, respectively. If the Magnus moment is large, one or the other of precession and nutation becomes unstable. The precessional and nutational frequencies are seen to be independent of gravity and side forces to second order, whereas the damping depends on these forces to the first order of approximation.

From the sign of each term in the expressions for λ we can ascertain whether given forces are stabilizing or destabilizing. This information is summarized in Table 3. For both nutation and precession, the destabilizing force must be greater than a certain minimum value to overcome the stabilizing influence of M_q and Z_w, respectively.

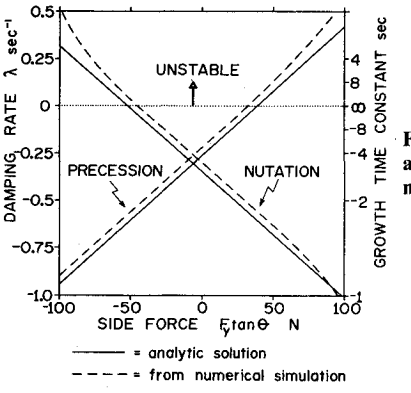

Fig. 2 Comparison of analytic solution with numerical simulation.

Substituting values for the parameters listed in Table 2 gives the following approximate expressions for the eigenvalues:

$$\omega_P = 4.5 \text{ rad/s}$$

$$\lambda_P = -0.269 + 0.0067F_y\tan\theta_0 - 0.039\sin\theta_0 \text{ s}^{-1}$$

$$\omega_N = 105 \text{ rad/s}$$

$$\lambda_N = -0.353 - 0.0067F_y\tan\theta_0 \text{ s}^{-1}$$

Terms involving the vertical force, F_z, have again been omitted as they are much smaller than the other terms.

We have plotted the damping rates, λ, Fig. 2. It is seen that the projectile is nutationally unstable for $F_y\tan\theta_0 < -60$N, and precessionally unstable for $F_y\tan\theta_0 > 40$N.

The θ,ϕ mode arises from the introduction of Eqs. (9) and (10) which allow θ and ϕ to vary. Note that this mode has a time constant of the order of 25 s and therefore does not vary significantly during the few seconds of validity of the present solution. Its physical significance is that it represents curvature of the trajectory.

V. Numerical Computations

There is always satisfaction when exact numerical calculations confirm an analytic treatment. This, plus the benefit of computer-plotted figures showing the nutational and precessional instabilities very clearly, are our excuses for presenting the results of some numerical simulations in this section.

We have written a simple six degree-of-freedom computer program to calculate the motion of a spinning projectile subjected to constant Earth-oriented control forces. The equations solved are Eqs. (1-4) plus the equations of motion in the x direction:

$$\dot{u} = \tfrac{1}{2}\rho V^2SC_x/m - qw + rv - g\sin\theta$$

$$\dot{p} = \tfrac{1}{2}\rho V^2SdC_{lp}pd/2VI_{xx}$$

with $C_X = -0.13$ and $C_{lp} = -0.025$. For completeness, we have also added a Magnus force term to Eqs. (1) and (3), with $C_{Y_{p\alpha}} = -1.5$. By running the program with and without these refinements, their contribution was found to be small.

The results of three runs of the program are given in Figs. (3-5). The shell parameters were set at the values given in Table 2, which apply to halfway down the downleg of a typical 105-mm shell trajectory. The elevation was set initially at -43 deg and the velocity at 250 m/s. During the 4s for which the trajectory was calculated, the mean elevation decreased to -48 deg and the velocity increased to 264 m/s; i.e., these values did not depart too much from the constant values assumed in the analytic solution. The numerical

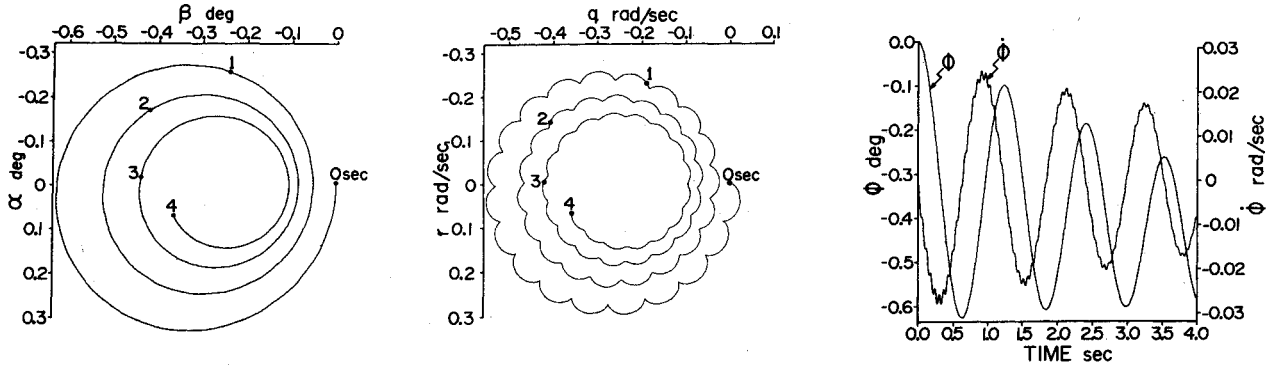

Fig. 3 Numerical simulation of motion of spinning projectile – no side forces.

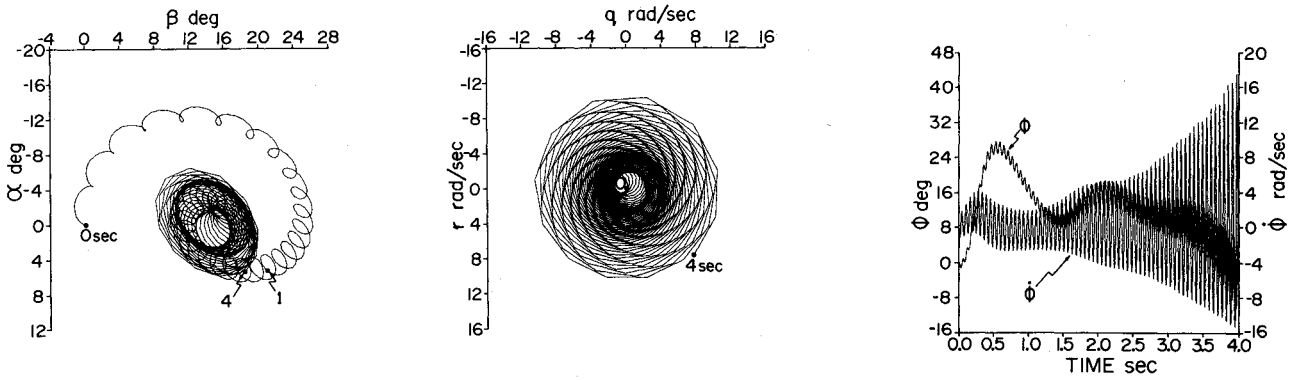

Fig. 4 Nutational instability produced by a horizontal side force to right.

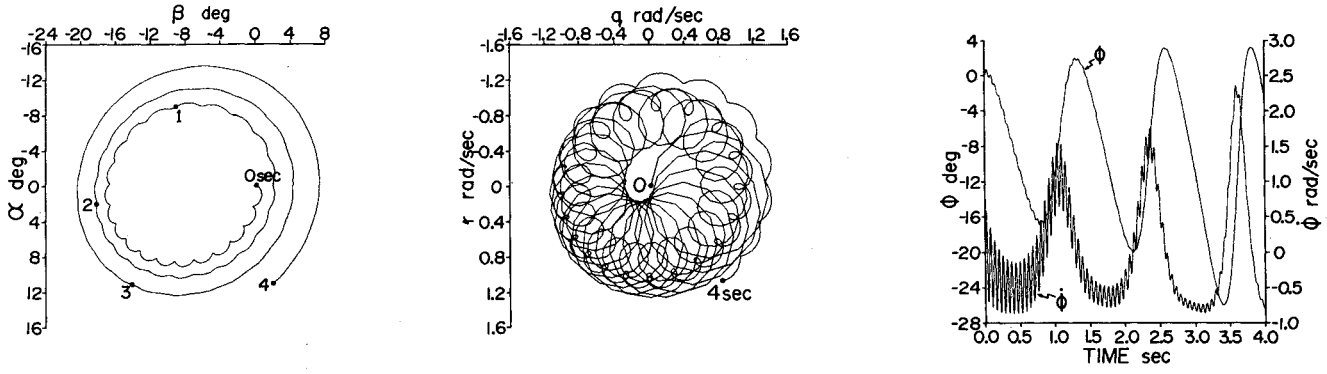

Fig. 5 Precessional instability produced by a horizontal side force to left.

calculations used a standard fourth-order Runge-Kutta routine. The time step was 0.0025 s; if it was much larger than this, nutation was found to be artifically damped.

Each figure shows angles of attack (β,α) and angular rates (q,r), together with values of $\dot{\phi}$ and its integral ϕ, the Euler roll angle of the nonspinning axes, as functions of time. These figures show very clearly the instabilities which were derived analytically. With no side forces acting (Fig. 3), both precessional and nutational modes are stable; a 100 N force to the right (Fig. 4) produces nutational instability and increases the precessional stability, whereas a 50 N force to the left (Fig. 5) gives precessional instability while increasing nutational stability.

The precessional and nutational modes are easily distinguished in Figs. 3-5, so estimates can be made of their frequency and damping. The results are plotted in Fig. 2. Comparison with the eigenvalues of the analytic treatment shows a systematic difference in λ of about 0.01/s. This is largely due to neglect of drag in the analytic treatment; Murphy[2] has shown that drag has a destabilizing effect, increasing λ by $\frac{1}{2}\rho V^2 S C_D/mV$ which equals 0.01/s for the present case. In addition to the systematic difference, there is a scatter of about 0.005/s, which is largely due to errors in estimating λ from the numerical simulations.

Finally, the numerical calculations enable us to see how valid our assumption was that the integrated residual roll, ϕ, was small. It is seen that although ϕ is very small ($\sim$0.01 rad) when there are no side forces, the approximation is only valid on short-time intervals for large side forces, where ϕ can approach 1 rad after a few seconds.

VI. Summary

The equations of motion of a spinning projectile have been written in nonspinning axes, whose angular velocity is (0, q, r), in which the directions of gravity and side forces are not constant but wobble in the complementary manner to the Eulerian roll angle of the nonspinning axes system. By assuming that this wobble is small, an analytic solution of the linearized equations is obtained whose general solution contains gravity and side forces in the damping term.

It is found that on the trajectory downleg, a horizontal side force to the right, applied at the nose, tends to stabilize precession and destabilize nutation, and a force to the lift tends to destabilize precession and stabilize nutation. The opposite occurs on the upleg. This means that a large enough side force (greater than about 40 N, for a 15 kg, 105-mm shell, when applied at the nose) will always cause the motion of the projectile to be dynamically unstable.

Gravity and side forces in the vertical plane have a much smaller effect on precessional and nutational stability than do horizontal side forces. For expected parameter values, these forces are unlikely to be large enough to overcome the stabilizing effects of the aerodynamic damping moment and normal force.

Numerical simulation of the motion of a projectile using a six degree-of-freedom computer program has confirmed these predictions of the analysis.

References

[1] Nicolaides, J.D., "Free Flight Dynamics," Tech. Note 100A, Dept. of Aerospace Engineering, University of Notre Dame, 1969.

[2] Murphy, C.H., "Free Flight Motion of Symmetric Missiles," Rept. 1216, Ballistic Research Laboratories, Aberdeen Proving Ground, Md., 1963.

[3] Regan, F.J. and Smith, J., "Aeroballistics of a Terminally Corrected Spinning Projectile," *Journal of Spacecraft*, Vol. 12, Dec. 1975, pp. 733-736.

[4] Kolk, W.R., *Modern Flight Dynamics*, Prentice Hall, Englewood Cliffs, N.J., 1961, p. 11.